NRC Publications Archive
Archives des publications du CNRC

Synthesis and characterization of carbon nanotube-reinforced epoxy : Correlation between viscosity and elastic modulus

Hubert, Pascal; Ashrafi, Behnam; Adhikari, Kamal; Meredith, James; Vengallatore, Srikar; Guan, Jingwen; Simard, Benoit

This publication could be one of several versions: author’s original, accepted manuscript or the publisher’s version. / La version de cette publication peut être l’une des suivantes : la version prépublication de l’auteur, la version acceptée du manuscrit ou la version de l’éditeur.
For the publisher’s version, please access the DOI link below./ Pour consulter la version de l’éditeur, utilisez le lien DOI ci-dessous.

Publisher’s version / Version de l'éditeur:
https://doi.org/10.1016/j.compscitech.2009.04.023
Composites Science and Technology, 69, 14, pp. 2274-2280, 2009-05-01

NRC Publications Record / Notice d'Archives des publications de CNRC:
https://nrc-publications.canada.ca/eng/view/object/?id=5b89d69f-b37c-47d3-8a6c-fada7d75411e
https://publications-cnrc.canada.ca/fra/voir/objet/?id=5b89d69f-b37c-47d3-8a6c-fada7d75411e

Access and use of this website and the material on it are subject to the Terms and Conditions set forth at
https://nrc-publications.canada.ca/eng/copyright
READ THESE TERMS AND CONDITIONS CAREFULLY BEFORE USING THIS WEBSITE.

L’accès à ce site Web et l’utilisation de son contenu sont assujettis aux conditions présentées dans le site
https://publications-cnrc.canada.ca/fra/droits
LISEZ CES CONDITIONS ATTENTIVEMENT AVANT D’UTILISER CE SITE WEB.

Questions? Contact the NRC Publications Archive team at PublicationsArchive-ArchivesPublications@nrc-cnrc.gc.ca. If you wish to email the authors directly, please see the first page of the publication for their contact information.

Vous avez des questions? Nous pouvons vous aider. Pour communiquer directement avec un auteur, consultez la première page de la revue dans laquelle son article a été publié afin de trouver ses coordonnées. Si vous n’arrivez pas à les repérer, communiquez avec nous à PublicationsArchive-ArchivesPublications@nrc-cnrc.gc.ca.

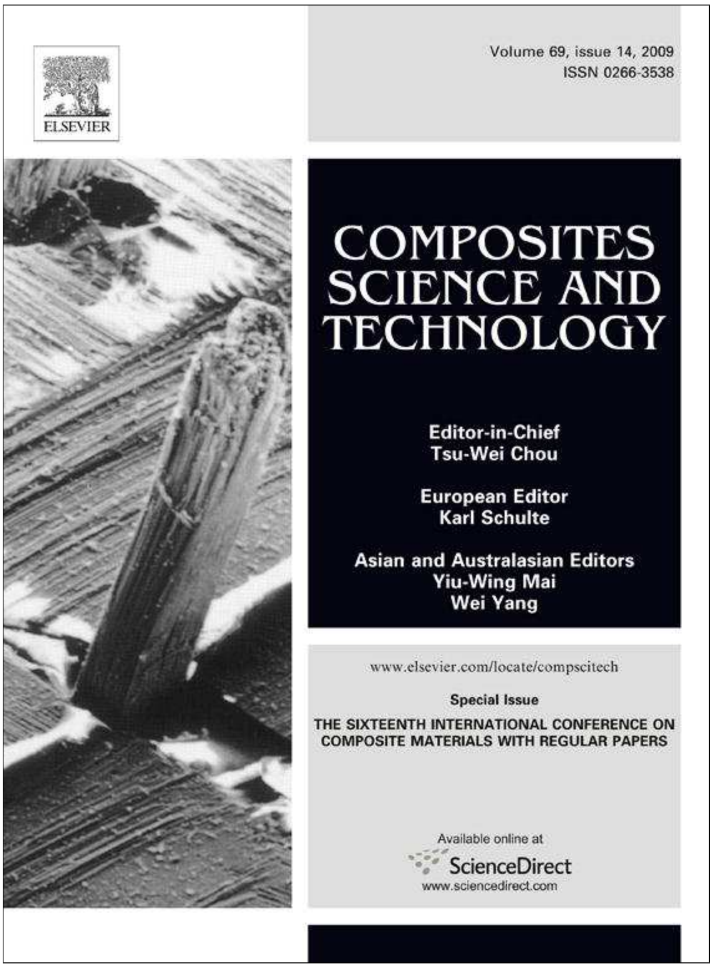

Composites Science and Technology 69 (2009) 2274–2280

Contents lists available at ScienceDirect

Composites Science and Technology

journal homepage: www.elsevier.com/locate/compscitech

Synthesis and characterization of carbon nanotube-reinforced epoxy: Correlation between viscosity and elastic modulus

Pascal Hubert [a,*], Behnam Ashrafi [a], Kamal Adhikari [a], James Meredith [a], Srikar Vengallatore [a], Jingwen Guan [b], Benoit Simard [b]

[a] *McGill University, Department of Mechanical Engineering, 817 Sherbrooke Street West, Montreal, QC, Canada H3A 2K6*
[b] *Molecular and Nanomaterial Architectures Group, Steacie Institute for Molecular Sciences, National Research Council of Canada, Ottawa, Ontario, Canada K1A 0R6*

ARTICLE INFO

Article history:
Received 19 June 2008
Received in revised form 3 April 2009
Accepted 30 April 2009
Available online 18 May 2009

Keywords:
A. Nanocomposites
A. Carbon nanotubes
B. Mechanical properties
D. Raman spectroscopy
D. Rheology
D. Thermogravimetric analysis (TGA)

ABSTRACT

We report the synthesis and characterization of nanocomposite thin films consisting of single-walled carbon nanotubes with different functionalization schemes dispersed in an epoxy matrix. The thermal, rheological, and mechanical properties of nanocomposite thin films were experimentally characterized to establish a relationship between processing and performance. The results from the rheological analysis confirmed that the nanotube type and functionalization strongly affect the resin viscosity during cure. A correlation between the rheological behaviour and the measured elastic properties was established. Nanotubes produced by plasma and functionalized with carboxyl group had the lowest influence on viscosity and led to the highest improvement in elastic properties. The measured increase in elastic modulus was consistent with predictions based on Mori–Tanaka micromechanics.

1. Introduction

Research on the synthesis and characterization of carbon nanotube (CNT)-reinforced polymer structures has produced a large and rich literature; several recent articles contain an excellent overview of these developments [1,2]. Much of the earlier work focused on the direct incorporation of the nanotubes as reinforcement fillers in the resin. These resins were then processed to fabricate films, fibres, or bulk composites with enhanced mechanical and other multifunctional properties. However, the measured enhancements in properties are significantly less than expected due to the difficulty of processing nanocomposites (especially in controlling alignment and dispersion, and in ensuring strong matrix–CNT interfaces). This difficulty is due, in part, to the effects of the nanotubes on the rheological and curing behaviour of the polymer. Specifically, the viscosity of the matrix can increase by orders of magnitude upon the addition of carbon nanotubes with large aspect ratios (length/diameter >500). The degree to which the viscosity is affected is highly dependent on the type and aspect ratio of the nanotubes [3], dispersion state [4], and functionalization [5]. Epoxy with functionalized nanotubes can exhibit a high degree of shear thinning behaviour compared to the neat resin [6]. Carbon nanotubes have shown to affect the cure behaviour of resin systems as well, and single-walled carbon nanotubes (SWCNT) in epoxy act as strong catalysts even at a loading of 5 wt.% [7]. The presence of CNT has led to an increase in the initial rate of reaction [8] and in the time to the maximum rate of reaction [9]. Thus, these effects cannot be ignored if one aims to have a full understanding of the processing of polymers in the presence of the nanotubes. As a step in that direction, this work presents a systematic experimental study that provides a foundation for developing chemistry-process–structure-property relationships for nanocomposite thin films. The focus of this work will be the investigation of the relationship between the rheological and mechanical properties of epoxy resins modified with SWCNT using different synthesis and functionalization methods.

2. Materials synthesis

2.1. Synthesis of single-walled carbon nanotube (SWCNT)

SWCNT were prepared using a highly efficient double-laser-oven technique [10] and a high throughput induction thermal plasma process [11]. For the laser-oven technique, an inert environment of flowing Argon (250 sccm) was maintained inside a 45 mm diameter quartz tube fitted with a Brewster window. A gas-inlet was positioned at one end, while a water-cooled collector (or an environmental sample chamber) and a pumping port were placed at the other. The pressure and temperature inside the

---

[*] Corresponding author. Tel.: +1 514 398 6303; fax: +1 514 398 7365.
E-mail address: pascal.hubert@mcgill.ca (P. Hubert).

0266-3538/$ - see front matter © 2009 Elsevier Ltd. All rights reserved.
doi:10.1016/j.compscitech.2009.04.023

quartz tube were maintained at 67 kPa and 1450 °C, respectively, throughout the process. Two types of lasers were employed in this process. The first was a nanosecond-pulsed Nd:YAG laser (Spectra-Physics Pro290–30) operating at 1064 nm (or 532 nm) and 30 Hz with a fluence of approximately 2 J cm^{-2}/pulse (and 1 J cm^{-2}/pulse), respectively. This laser was setup for the purpose of vaporizing the targets (graphite doped with 0.6 at.% each of cobalt and nickel). The second laser used in this process was a Nd:YAG laser (Spectra-Physics Tornado S240-TN50–106Q), operating at either continuous wave or 20 kHz, at a wavelength of 1064 nm and measured average powers of 50 W and 48 W, respectively. This laser was used to alter the rate of cooling of the condensing plume generated by the vaporizing laser. The product of this process contained SWCNT (70 wt.%), metal catalyst contamination (6 wt.%), and other impurities including amorphous and graphitic carbon particles. Subsequently, the as-produced SWCNT were subjected to a purification process to remove these impurities. Briefly, this process relies on cycles of solvent extraction, floatation and precipitation. Besides its simplicity and scalability, an important feature of the procedure was that it did not damage the SWCNT, as will be shown later. The specific details and techniques of the purification procedure are in preparation and will be published elsewhere.

2.2. SWCNT and epoxy integration

The carbon nanotubes manufactured by the laser process were functionalized using 4-aminobenzyl alcohol through diazonium reactions following the procedure shown in Scheme 1 [12] in Fig. 1 (designated as "Alkoxy Laser"). Alternately, carboxyl groups were introduced using the rapid functionalization method developed in our laboratory, shown in Scheme 2 [13] in Fig. 1 (designated as "Carboxyl Laser"). The underlying motivation for functionalization was to aid in the debundling and dispersion of the nanotube during composite processing. For the plasma produced SWCNT, only carboxyl functionalization was used (designated "Carboxyl USP").

The matrix used in this study was a standard aerospace grade epoxy, Araldite® MY0510 epoxy (Huntsman), which was cured with 4,4-Diaminodiphenyl Sulphone (DDS) as the hardener. The integration of hydroxy-functionalized SWCNT into MY0510 is described in Scheme 3 (Fig. 1). Briefly, the hydroxy group was first deprotonated with sodium metal in THF under nitrogen atmosphere to form an alkoxy group, a strong nucleophilic agent. Following nucleophilic attacks on the epoxy groups, C–O covalent bonds are formed between the epoxy resin and the SWCNT. In the absence of moisture, the reaction would continue and cross-link the resin until all the epoxide groups are transformed. For this study, the cross-link reaction was stopped after 2 h by sparging air until most of the solvent was removed. Finally, the viscous resin mixture was placed in a vacuum oven at 100 °C and <100 kPa overnight to complete removal of the solvent. Carboxyl-functionalized SWCNT can be covalently anchored to the MY0510 resin through esterification reactions between the carboxylic and epoxide groups, as shown in Scheme 4 (Fig. 1). Here, a well-dispersed sus-

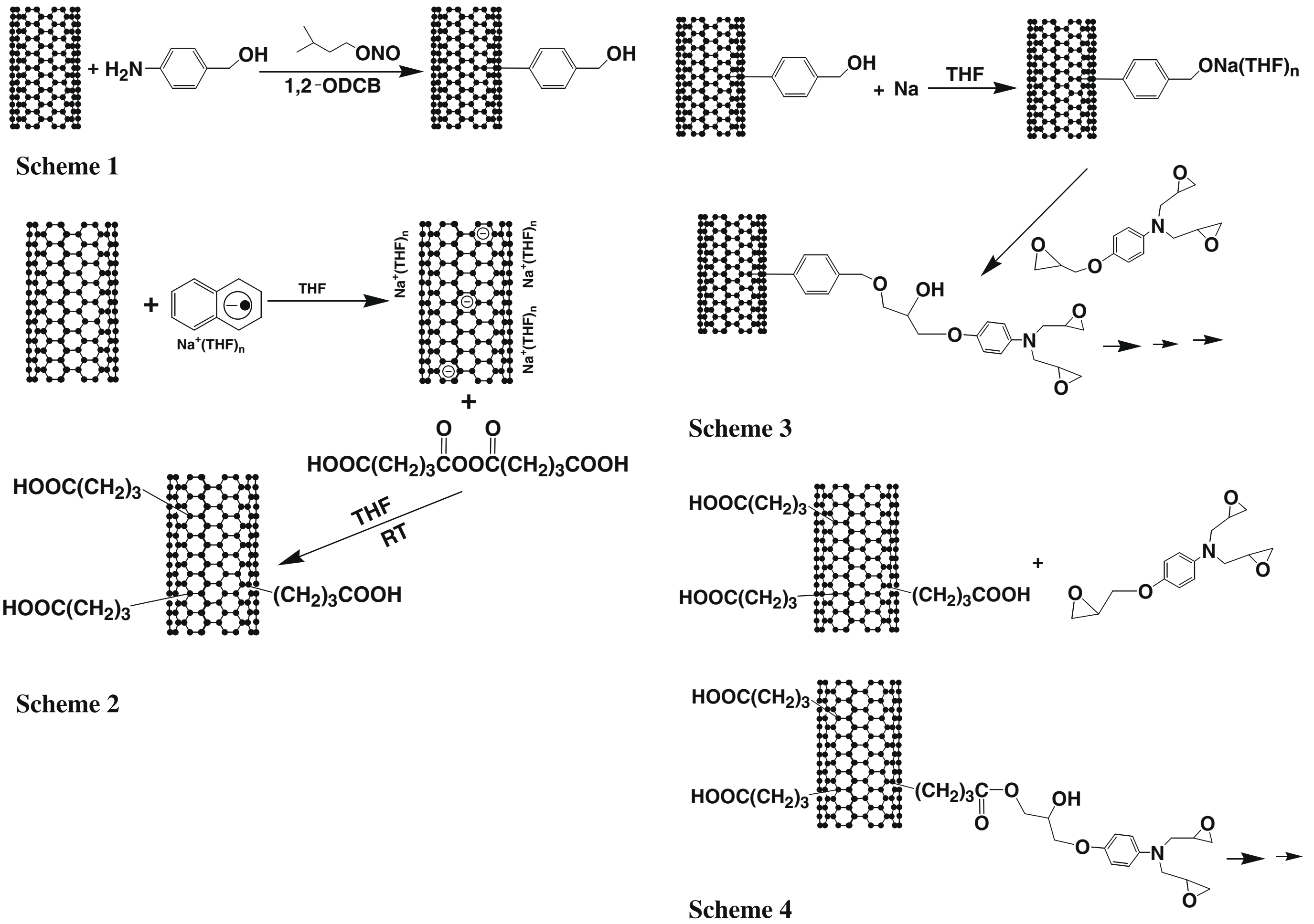

Fig. 1. Different schemes for chemical integration of epoxy and SWCNT. Scheme 1: Alkoxy functionalization of SWCNT through diazonium reactions. Scheme 2: Carboxyl functionalization of SWCNT by the rapid functionalization method. Scheme 3: Anchoring of MY0510 onto the alkoxy-functionalized SWCNT. Scheme 4: Anchoring of MY0510 onto carboxyl-functionalized SWCNT through esterification.

pension of Carboxyl-SWCNT in THF was mixed with MY0510 by shear-mixing and after 2 h air was sparged to remove the solvent. The composite was then placed in a vacuum oven and maintained at 100 °C and under vacuum (30 InHg) overnight.

3. Material characterization

3.1. SEM characterization

Scanning electron micrographs were obtained using a Hitachi S-4800 FE microscope, operating at 1.2 kV, at a distance of 3 mm. Samples were prepared by pipetting a few drops of a suspension of SWCNT in methanol onto an aluminum SEM sample stub with a disposable Pasteur glass pipet. Fig. 2 shows micrographs of the as-produced and purified SWCNT. We estimate that the SWCNT content in the purified material is >90%.

3.2. Raman characterization

Raman spectra were recorded on a custom built spectrometer consisting of a Spectra-Physics Lasers (model: 277-GA04) generator, and a WiTec confocal microscope fibre coupled to an Acton 2500i spectrograph fitted with a Roper Scientific CCD array detector. Measurements were carried out using 514.5 nm excitation attenuated to have a power density well below 2 kW cm^{-2} at the sample to avoid laser heating effects. Raman samples were prepared by sonicating a few mg of SWCNT in a few ml of methanol in a sonication bath for 15 min. Fig. 3 compares Raman spectra of the as-produced and purified SWCNT. The D-band of the purified SWCNT exhibits a smaller intensity than the corresponding band of the as-produced nanotubes. This demonstrates that the purification technique did not damage the structure of SWCNT.

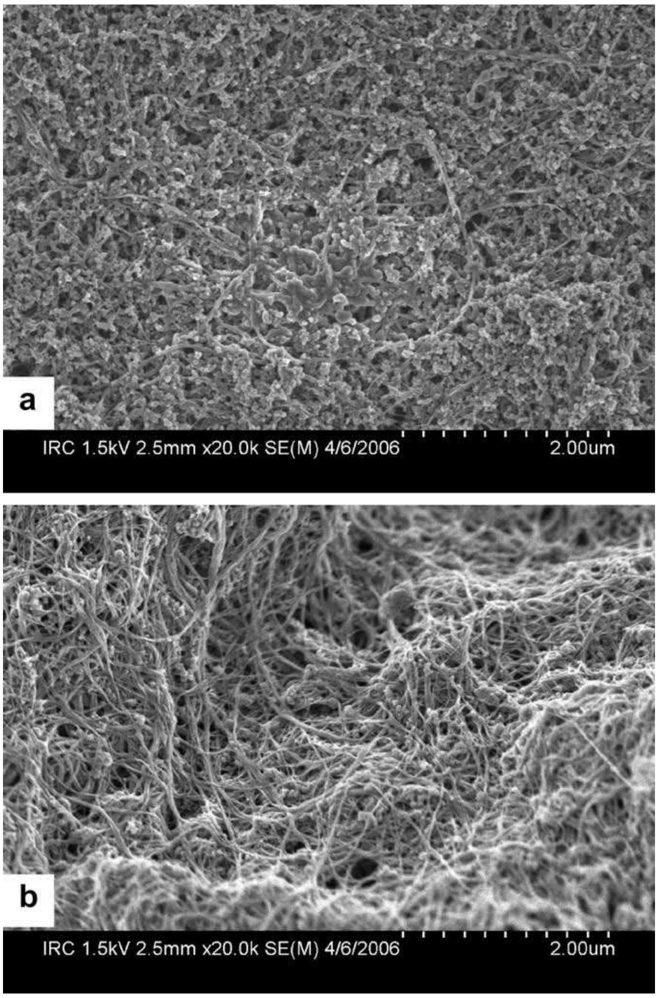

Fig. 2. (a) SEM image of as-produced SWCNT and (b) SEM image of purified SWCNT.

3.3. Thermogravimetric characterization

Thermogravimetric analysis (TGA) indicates a structural modification of the epoxy system when subjected to a compatible nanotube functional group. The TGA tests were performed with a Perkin–Elmer TGA7 unit, and three calibration routines were performed prior to the characterization of the nanocomposite. The first routine was performed to match the temperatures of the furnace and thermocouple, the second was a two-standard calibration using nickel and iron to calibrate the Curie point, and the third was a mass calibration of the unit, which was performed using a 100 mg standard.

The TGA experiments were performed on four sets of specimens: MY0510 (neat), MY0510/DDS, SWCNT/MY0510 (with 0.2 wt.% of SWCNT), and SWCNT/MY0510/DDS (with 0.125 wt.% of SWCNT). The MY0510 was poured into the specimen holder as received, but the MY0510/DDS, SWCNT/MY0510 and SWCNT/MY0510/DDS specimens were stirred manually using a glass stirrer for 30 min to ensure homogeneity before being poured into the specimen holder. For the specimens containing DDS, the epoxy and hardener were mixed in a ratio of five parts epoxy to three parts of hardener, as recommended by the manufacturer. The TGA tests were performed by heating the specimen in air to a maximum temperature of 800 °C at a rate of 20 °C/min.

Figs. 4 and 5 show the weight loss as a function of temperature for the neat resin and various SWCNT–reinforced nanocomposites. The data in Fig. 4 are for epoxy and nanocomposite systems without the use of the hardener DDS, and show that the nanotubes affect the thermal degradation profile, particularly after 350 °C. Therefore, the nanotubes act as mild curing agents which react with the epoxy groups. The results of a similar comparison on specimen containing DDS are shown in Fig. 5. This graph confirms that DDS improves the thermal stability of MY0510, and that the nanotubes lead to an additional increase in stability after 350 °C.

3.4. Rheological characterization

Rheological tests were performed on MY510/DDS and SWCNT/MY0510/DDS specimens using a TA Instruments AR2000 rheome-

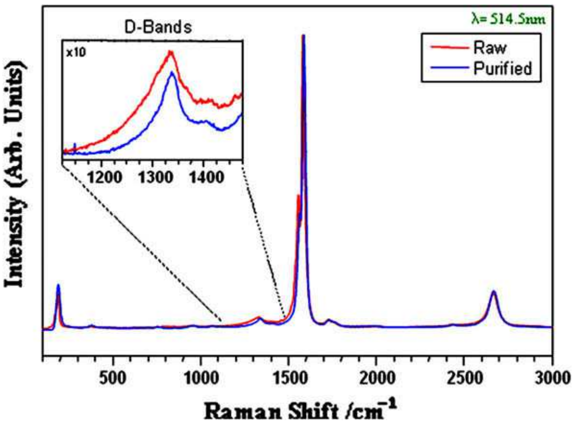

Fig. 3. Raman spectra of as-produced and purified SWCNT produced by the laser-oven method.

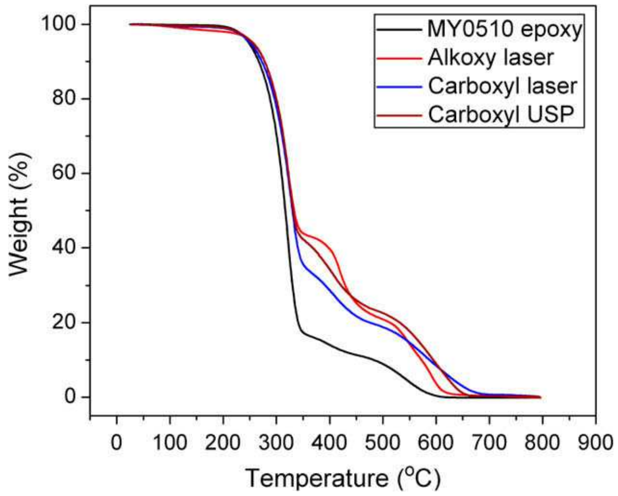

Fig. 4. Weight loss as a function of temperature for MY0510 epoxy and for MY0510-matrix nanocomposite containing 0.2 wt.% SWCNT. The nanotubes were produced by the laser process (and functionalized with alkoxy and carboxyl groups) and by the plasma process (and functionalized with carboxyl groups), as indicated.

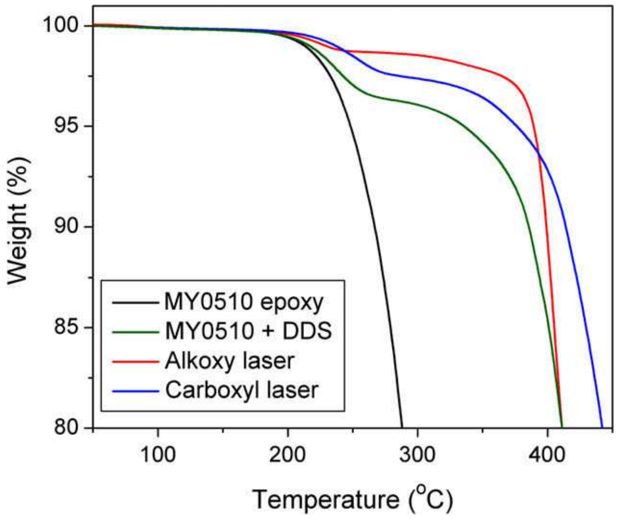

Fig. 5. Weight loss as a function of temperature for MY0510 epoxy (with and without DDS), and for MY0510/DDS nanocomposite containing 0.125 wt.% SWCNT. The nanotubes were produced by the laser process and functionalized with alkoxy and carboxyl groups as indicated.

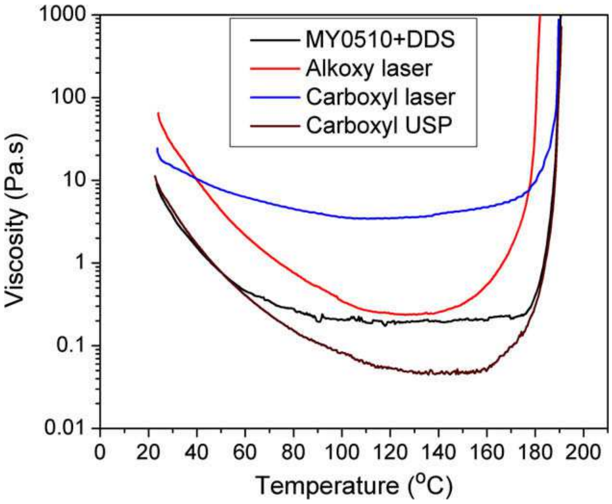

Fig. 6. Temperature dependence of viscosity for MY0510 epoxy (with DDS hardener). The effects of adding 0.125 wt.% SWCNT on viscosity are indicated. The red and blue curves correspond to nanotubes produced by the laser process and functionalized with alkoxy and carboxyl groups, respectively. The brown curve corresponds to nanotubes produced by the plasma process and functionalized with carboxyl groups. (For interpretation of the references to colour in this figure legend, the reader is referred to the web version of this article.)

ter with 40 mm parallel plates. The sample gap size was kept in the range of 500–1000 μm (volume of 0.628–1.257 ml) per sample. Dynamic temperature tests (oscillatory temperature ramp) were performed on the nanocomposite mixture to observe the variations in the viscosity profile of the resins with temperature. The test was performed from room temperature to 250 °C at a ramp rate of 3 °C/min. The control variable of 12% strain was used with the sampling rate set at 1 point every 10 s at the frequency of 1 Hz. The post-experiment step set the temperature back to 25 °C. Fig. 6 presents the viscosity measured during cure as a function of temperature. The results clearly illustrate the effect of a dilute concentration of SWCNT on the rheological behaviour of the resin. The nanotubes produced by the laser process (and functionalized with alkoxy and carboxyl groups) increased the viscosity of the epoxy by an order of magnitude at room temperature (25 °C). Further, the difference in viscosity between the neat epoxy and the mixture containing carboxyl-functionalized SWCNT is almost two orders of magnitude at 100 °C. In contrast, the SWCNT produced by the plasma process (and functionalized using carboxyl group) led to relatively little change in the viscosity of the epoxy at room temperature. However, the epoxy reinforced with this type of nanotubes showed a significant *decrease* in its viscosity over a temperature range of 80–150 °C. The plasma process is known to produce nanotubes of shorter length in comparison with the laser process, and this change in structural characteristic is assumed to be the primary cause for the observed differences in the viscosity.

4. Experimental characterization of mechanical properties

The elastic properties of nanocomposite thin films were assessed using a nanoindenter-based bending test. This method is essentially a bending test performed on a clamped circular plate subjected to a central point load. In practice, the test was performed by employing a commercial nanoindenter (TriboIndenter, Hysitron) to apply loads and measure displacements with resolution of micronewtons and nanometers, respectively. Fig. 7a shows an exploded schematic diagram of the fixture used for testing. Considering a clamped circular film of thickness h and radius a that is loaded at the center using a spherical indenter (Fig. 7b), the applied load P leads to a deflection that contains two components: deformation due to bending of the plate (δ_P) and deflection due to the local indentation at the point of contact with the indenter (δ_C). The total displacement, δ_T, measured by a nanoindenter, is simply the sum of these two deformations and hence:

$$\delta_T = \delta_C + \delta_P \tag{1}$$

The displacement of the center of a circular plate clamped at its edge and loaded with a point load at its center is given by Timoshenko's plate theory [14]:

$$\delta_P = \frac{3(1-\nu^2)}{4\pi E}\frac{a^2}{h^3}P \tag{2}$$

Here, E and ν are, respectively, Young's modulus and Poisson's ratio of the plate. For the second deformation, as a first approximation, the contact indentation was assessed using Hertzian contact mechanics. The depth of indentation (δ_C) caused by a spherical tip on an elastic half-space is given by:

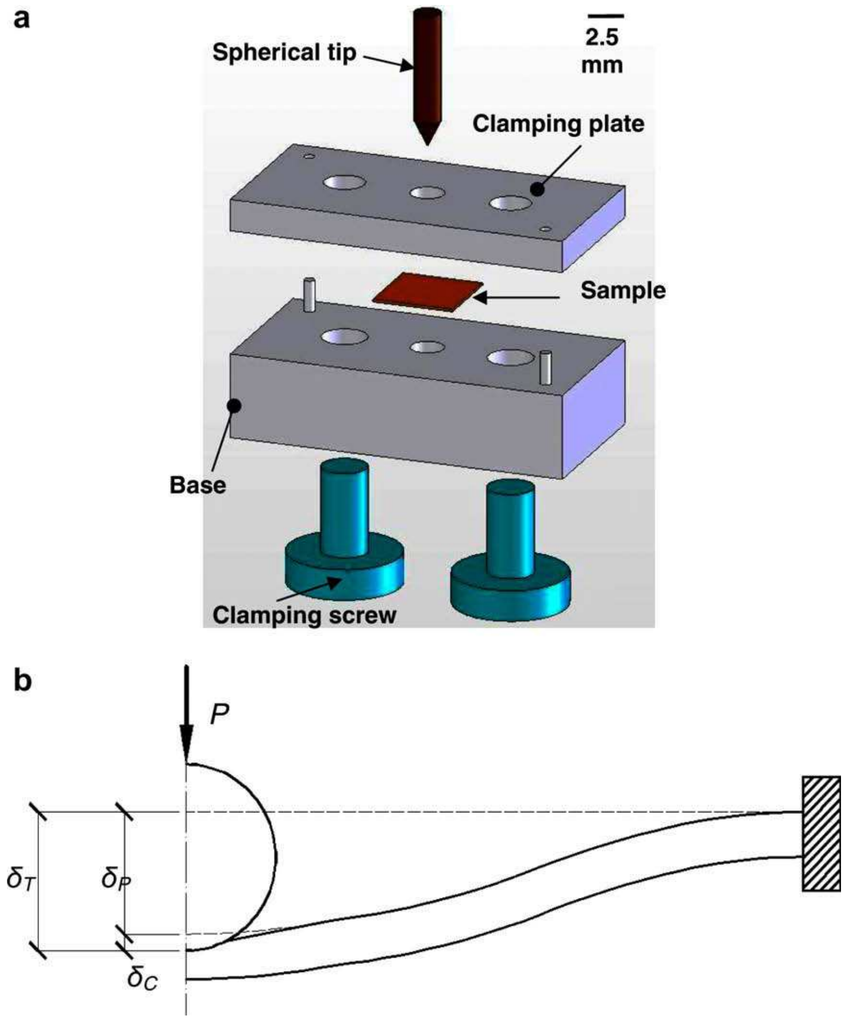

Fig. 7. (a) A schematic design of the bending fixture and its components. (b) Contact indentation (δ_C) and plate deflection (δ_P) as a result of load P.

$$\delta_C = \sqrt[3]{\frac{9}{16}\frac{P^2}{RE_r^2}} \tag{3}$$

where R is the tip radius and E_r is the reduced modulus (combined modulus) defined as:

$$\frac{1}{E_r} = \frac{1-\nu^2}{E} + \frac{1-\nu_I^2}{E_I} \tag{4}$$

Here E_I and ν_I are the known values of the elastic constants for the indenter. By substituting for δ_P and δ_C in Eq. (1) from Eqs. (2) and (3), we obtain:

$$\delta_T = \sqrt[3]{\frac{9}{16}\frac{P^2}{RE_r^2}} + \frac{3(1-\nu^2)}{4\pi E}\frac{a^2}{h^3}P \tag{5}$$

A detailed description of the development and validation of this test method, experimental protocols, and data analysis procedures are described elsewhere [15]. In implementing this test, care must be exercised to ensure that the deformation is in the bending regime. In general, a plate deflection of less than 5% of the film thickness guarantees a pure bending behaviour of the film [16]. Fig. 8 shows the ratio of contact indentation to plate deformation (δ_C:δ_P) on a logarithmic scale as a function of film thickness, under the condition that the maximum permissible force $P_{\max}$ is applied in the plate deformation regime. Here, the radii of the spherical indenter (R) and circular plate are, respectively, equal to 100 µm and 1.25 mm to match the experimental setup. As long as the film is characterized with the maximum plate-regime force, the displacement ratio is not dependent on the film's Young's modulus (thick curve). However, since the force that can be applied using the TriboIndenter is

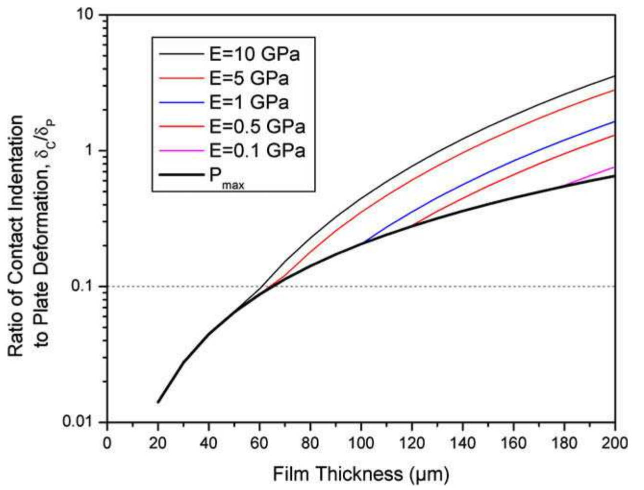

Fig. 8. Contact-to-plate displacement ratio as a function of film thickness for different values of the elastic modulus.

Table 1
Elastic properties of MY0510 polymer and polymer nanocomposites.

	CNT (wt.%)	*E* (GPa)	Percentage change	
			Experiments (%)	Mori–Tanaka (%)
Neat resin	–	3.4 ± 0.2	–	–
Carboxyl Laser	0.125	2.9 ± 0.3	−15	3.75
Alkoxy Laser	0.125	3.5 ± 0.2	3	3.75
Carboxyl USP-1	0.125	3.6 ± 0.2	6	3.75
Carboxyl USP-2	0.250	3.3 ± 0.3	−3	7.5
Carboxyl USP-3	1.000	4.2 ± 0.2	24	30

limited to a maximum force of 15 mN, it is not possible to reach the maximum plate-regime force with thicker films. As a result, the displacement ratio is a function of the Young's modulus of the film.

Thin films of MY0510 epoxy and epoxy-reinforced nanocomposites were prepared in the form of uniform thin films with thickness ranging from 25 to 60 μm. This was accomplished by curing the films between two glass substrates. This range of thicknesses results in $\delta_C{:}\delta_P < 0.1$ (Fig. 8), so that the films were characterized mainly based on their plate deformation. Finally, the elastic modulus was obtained from the measured load–displacement curves by using Eq. (5) and assuming a value of 0.4 for the Poisson's ratio of the films.

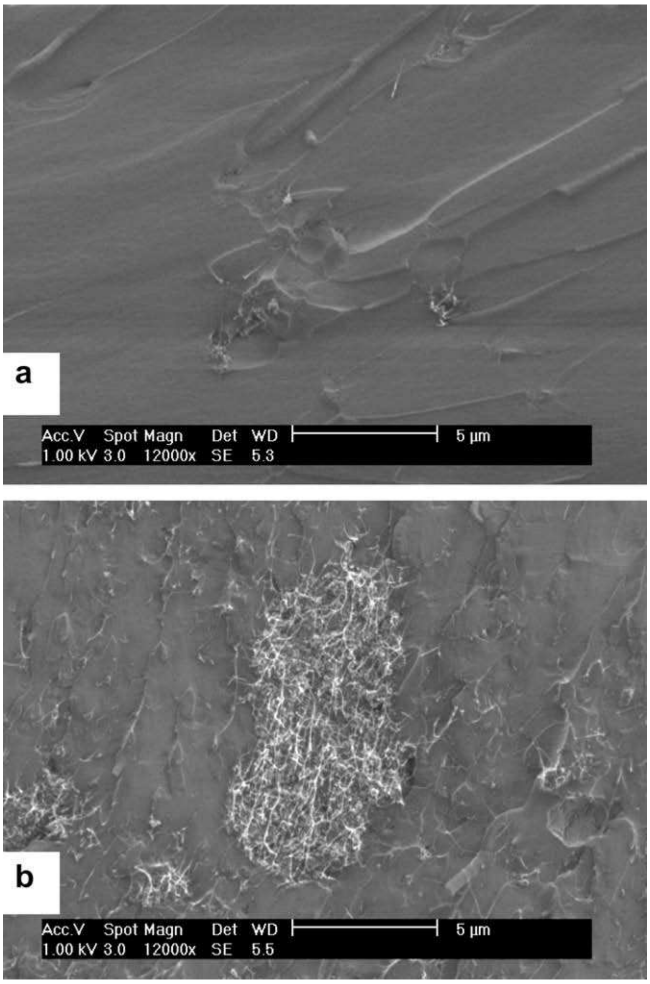

Fig. 9. SEM images of (a) pure epoxy and (b) Carboxyl USP-3 nanocomposite taken over the fractured cross-sections of thin films. Presence of individual SWCNT ropes and small SWCNT agglomerates can be observed within the nanocomposite samples.

The results from several sets of tests on MY0510 epoxy thin films, and different nanotube-reinforced epoxy thin films, are cataloged in Table 1. These values represent the average over four different films for each case. For comparison, the flexural modulus of MY0510 epoxy is reported to be 3.4 GPa by the manufacturer (Huntsman). The last column in this table shows the change in the elastic modulus of the nanocomposite using the neat epoxy as the baseline. The measured change (in percentage) is compared with the change computed using the Mori–Tanaka method [17], assuming that the reinforcing agents are arrays of SWCNT with perfectly-random orientation within the matrix. The predicted change for specimens with low loading of SWCNT (in the range of 0.125–0.25%) is only 3.75%, which is below the resolution of this technique. However, a significant increase of 24% was measured in the elastic modulus for the specimen reinforced with 1% of plasma-produced, carboxyl-functionalized SWCNT. This increase can be placed in context by noting that the predictions of the Mori–Tanaka calculation for random composites [17] (which assumes perfect bonding between reinforcement and matrix) is 30% for this specimen. Fig. 9 shows SEM images of the fractured cross-sectional areas of both pure epoxy and Carboxyl USP-3 (1 wt.% SWCNT) films. Individual ropes of SWCNT with diameters of tens of nanometers can be seen all over the cross-sectional areas of nanocomposite films. However, the presence of small SWCNT agglomerates of a few micrometer can also be observed in these films as illustrated in Fig. 9b, demonstrating non-uniform dispersion of inclusions inside the matrix.

5. Summary

This paper presented the results from an experimental study of the rheological and mechanical properties of nanocomposite thin films. The films consisted of a standard epoxy (MY0510) reinforced with different types of single-walled carbon nanotubes (produced by laser and plasma-based techniques, and functionalized with alkoxy and carboxyl groups). A low viscosity during cure was correlated with improved mechanical properties in thin-film form. This correlation is attributed to the enhanced ease of processing due to the reduced viscosity of these specimens. The SWCNT produced using the laser process exhibited a length to diameter aspect ratio exceeding 10,000. In comparison, the aspect ratio of the SWCNT obtained from the plasma process was ∼1000. The former is considerably more difficult to disperse in the epoxy matrix than the latter. Specimens with nanotube loadings of up to 1% were processed into thin films using the plasma SWCNT in an epoxy matrix. The elastic modulus of this material increased by 24% in comparison with the neat epoxy. This improvement is consistent with expectations based on micromechanical analysis using the Mori–Tanaka theory.

Acknowledgments

Financial support from the Natural Sciences and Engineering Research Council (NSERC) of Canada through the Discovery Grants Program and a PGSD scholarship are gratefully acknowledged. We are also grateful to Mr. Gordon Chan of NRC-IRC and Mr. David Chow of NRC-IAR for the recording of SEM images, and Drs. Chris Kingston and Yadienka Martinez-Rubi for the recording of the Raman spectra and the preparation of the carboxyl-functionalized SWCNT, respectively.

References

[1] Coleman JN, Khan U, Blau WJ, Gun'ko YK. Small but strong: a review of the mechanical properties of carbon nanotube–polymer composites. Carbon 2006;44:1624–52.

[2] Thostenson ET, Li C, Chou TW. Nanocomposites in context. Compos Sci Technol 2005;65:491–516.

[3] Sung YT, Han MS, Song KH, Jung JW, Lee HS, Kum CK, et al. Rheological and electrical properties of polycarbonate/multi-walled carbon nanotube composites. Polymer 2006;47(12):4434–9.

[4] Kim JA, Seong DG, Kang TJ, Youn JR. Effects of surface modification on rheological and mechanical properties of CNT/epoxy composites. Carbon 2006;44(10):1898–905.

[5] Song YS, Youn JR. Influence of dispersion states of carbon nanotubes on physical properties of epoxy nanocomposites. Carbon 2005;43(7):1378–85.

[6] Mitchell CA, Bahr JL, Arepalli S, Tour JM, Krishnamoorti R. Dispersion of functionalized carbon nanotubes in polystyrene. Macromolecules 2002;35(23):8825–30.

[7] Puglia D, Valentini L, Kenny JM. Analysis of the cure reaction of carbon nanotubes/epoxy resin composites through thermal analysis and Raman spectroscopy. J Appl Polym Sci 2003;88(2):452–8.

[8] Xie H, Liu B, Yuan Z, Shen J, Cheng R. Cure kinetics of carbon nanotube/tetrafunctional epoxy nanocomposites by isothermal differential scanning calorimetry. J Polym Sci: Part B: Polym Phys 2004;42(20):3701–12.

[9] Wang S, Liang Z, Liu T, Wang B, Zhang C. Effective amino-functionalization of carbon nanotubes for reinforcing epoxy polymer composites. Nanotechnology 2006;17(6):1551–7.

[10] Kingston CT, Jakubek ZJ, Dénommée S, Simard B. Efficient laser synthesis of single-walled carbon nanotubes through laser heating of the condensing vaporization plume. Carbon 2004;42(8–9):1657–64.

[11] Kim KS, Cota-Sanchez G, Kingston CT, Imris M, Simard B, Soucy G. Large-scale production of single walled carbon nanotubes by induction thermal plasma. J Phys D Appl Phys 2007;40:2375–87.

[12] Dyke CA, Tour JM. Solvent-free functionalization of carbon nanotubes. J Am Chem Soc 2003;125:1156–7.

[13] Martinez-Rubi Y, Guan JW, Lin S, Scriver C, Sturgeon RE, Simard B. Rapid, controllable and scalable covalent functionalization of single-walled carbon nanotubes at room temperature. Chem Commun 2007;48:5146–8.

[14] Timoshenko S. Theory of plates and shells. 2nd ed. McGraw-Hill; 1959.

[15] Ashrafi B. Theoretical and experimental investigations of elastic properties of carbon nanotube-reinforced polymer thin films. Mechanical Engineering. Ph.D. Thesis, McGill, Montreal; 2008.

[16] Komaragiri U, Begley MR, Simmonds JG. The mechanical response of freestanding circular elastic films under point and pressure loads. J Appl Mech 2005;72:203–12.

[17] Ashrafi B, Hubert P, Vengallatore S. Carbon nanotube-reinforced composites as structural materials for microactuators in microelectromechanical systems. Nanotechnology 2006;17:4895–903.